FEASIBILITY STUDY OF SUPERCONDUCTING LSM LAUNCHER SYSTEM FOR PRACTICAL H-II ROCKET

Kinjiro Yoshida*, Takeshi Kawanami**

* Department of Electrical and Electronic System Engineering,
Graduate School of Information Science and Electrical Engineering, Kyushu University
10-1 6-chome Hakozaki Higashi-ku Fukuoka ,812-8581 Japan

** Tokyo Electric Power Co., Inc.

SUMMARY

A practical feasibility study on superconducting linear synchronous motor (LSM) rocket launcher system for H-II rocket is presented on a basis of dynamic simulations of electric power energy, efficiency and power factor as well as ascending motions of the launcher and rocket. To decrease vastly maximum reactive power per section and to improve electrical efficiency and power factor, four-power-supply (A-B-C-D) system is introduced to shorten one section length as small as possible. It is made clear that the LSM rocket launcher system can obtain very high energy-efficiency of 94 %. It is found from very large instantaneous power at a peak speed and relatively low required-energy that initial cost is very high but operating cost is very low.

INTRODUCTION

We proposed a vertical type superconducting linear synchronous motor (LSM) rocket launcher system of which four acceleration guideways with double-layer armature windings are arranged symmetrically along a shaft of about 1,500 m under the ground. From our feasibility study, it is found that the linear launcher made the rocket attain the speed of 700 km/h at the height of 100 m above the ground, where the payload could be increased more than 15 % by substituting it for the first acceleration rocket. The linear launcher is brought to a stop at the ground surface by a quick control of deceleration. Superconducting LSM rocket launcher system was simulated to operate in an attractive-mode, controlling the Coriolis force [1]. Dynamics simulations of ascending the 4-ton-launcher with 1-ton-rocket were obtained to meet the same acceleration pattern of quick acceleration and deceleration rates as that of the repulsive-mode operation used in our previous papers [2], [3]. Electrical dynamics were simulated for electric powers, efficiency and power factor as well as ascending motions of launcher and rocket. It has been found that an optimal design of the 60-sections-length power supply system enable the system to obtain high efficiency and power factor [1].

This paper presents electromechanical dynamics simulations of ascending the launcher for H-II rocket of practical size (length 48m , diameter 4m and weight 256 ton) which meet the same acceleration pattern of quick acceleration and deceleration rates as that of the attractive-mode operation used in our previous papers. After the rocket is released at a peak speed of about 900 km/h, the linear launcher is stopped for a very short time of 5 seconds by a rapid control of deceleration. To decrease vastly maximum reactive power per section and to improve electrical efficiency and power factor, four-power-supply (A-B-C-D) system is introduced to shorten one section length as small as possible. Electric power, energy, efficiency and power factor are evaluated qualitatively for more practical feasibility study. It is made clear that the LSM rocket launcher system with four-power-supply (A-B-C-D) system can obtain very high energy-efficiency of 94%.

SUPERCONDUCTING LSM ROCKET LAUNCHER SYSTEM FOR H-II ROCKET

Figure 1 shows a concept of a large-scale superconducting LSM-controlled rocket launcher system

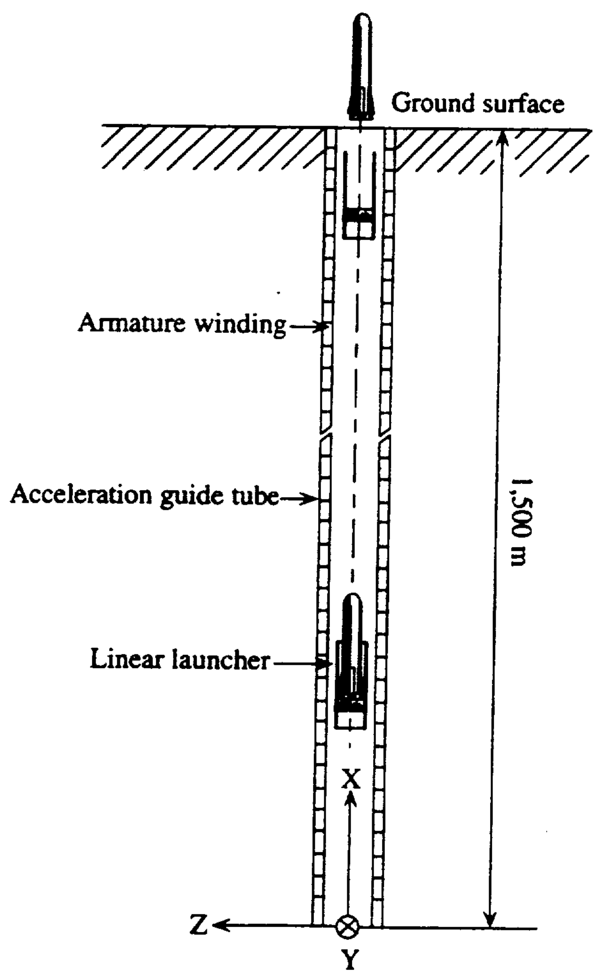

Figure 1. Vertical type superconducting-LSM controlled rocket laucher system for H-II rocket.

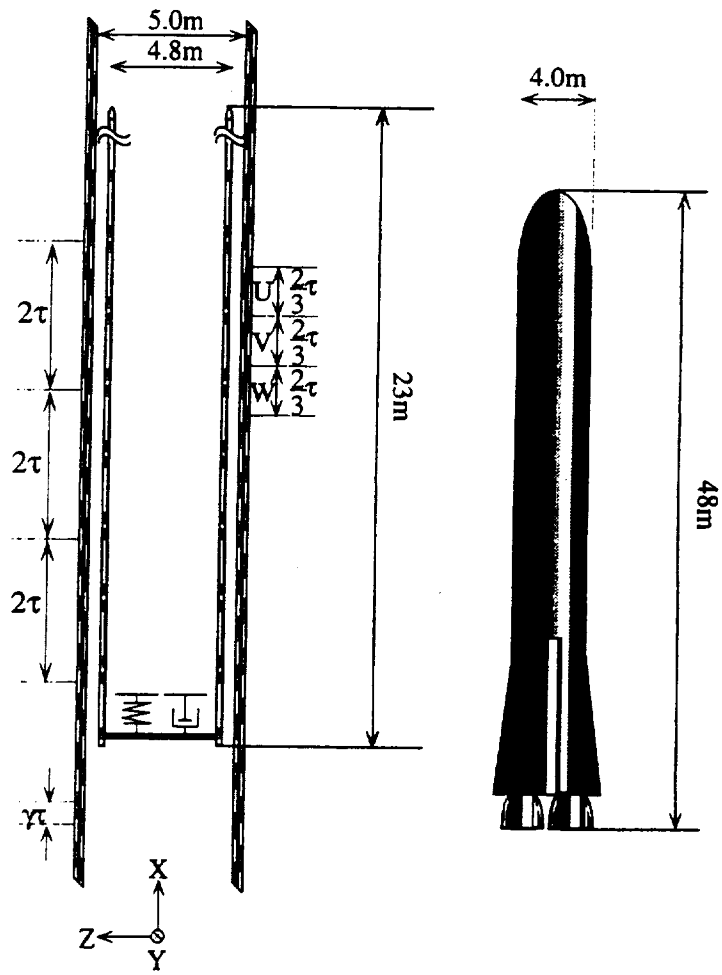

Figure 2. Acceleration guide tube of LSM armature and rocket laucher with superconducting magnets, and H-II rocket.

for H-II rocket, which has the acceleration guide tube of about 1,500 m deep under the ground. The concept is based on our theoretical work on a superconducting LSM-controlled ground-based zero-gravity facility with the drop shaft of about 800 m [4]. In Fig. 1, the LSM armature-windings which are installed all along the acceleration guide tube are used to drive and guide the linear launcher.

Figure 2 shows double-layer windings of the LSM armature which are composed of inside and outside coils, and the linear launcher on which the rocket is mounted through the use of passive suspension. The superconducting magnets are arranged with two poles facing the armature-windings in the front and rear portions of the linear launcher vehicle.

ASCENDING AND GUIDANCE MOTION CONTROL OF LINEAR LAUNCHER SYSTEM FOR H-II ROCKET

The linear launcher is accelerated to a peak speed, with the H-II rocket, and after releasing the rocket, it is decelerated with no-load to be brought to rest at the end of guide tube near the earth surface. On the other hand, during the acceleration phase, the rocket is fixed to the launcher through a passive suspension, but after separation from the launcher, it ascends freely in the guide tube. According to the armature-current control method proposed in Reference [1], the ascending motions in the X-direction of the launcher and the rocket are controlled together with the guidance motions in the Y-Z plane. When the Z-axis is assumed to be in an eastward direction, the Coriolis force can be taken into account as an external disturbance force in the Z-directed motions of the linear launcher and the rocket.

After the rocket is released from the launcher and takes off with a high initial-speed, the rocket continues to ascend with no control subject to the Coriolis force in the Z-direction under the force of gravity in the X-direction.

The effective values of armature-currents in four LSM systems are controlled independently for the launcher to meet the command acceleration pattern. The linear launcher should be controlled simultaneously to ascend at the synchronous speed V_{x0} of the travelling magnetic field, by producing total thrust force F_x due to all the four LSM-systems. The mechanical load-angle is controlled for all the four LSM's to produce the sufficiently strong attractive force due to the resultant guidance forces F_Y and F_Z. When the launcher receives any disturbance forces in the Y- and Z-directions, the LSM guidance forces can compensate them automatically and keep it at the center of the four LSM's.

ANALYSIS OF ELECTRICAL DYNAMICS

By applying vector analysis in the 3-phase armature-windings connected to satisfy the condition of $i_u+i_v+i_w=0$, the terminal voltage per phase $\dot{V}$ is derived in the following vector expression [1]:

$$\dot{V} = 2R\dot{I} + 2j\omega\left(L - M_2 + M_4 - \frac{M_5 + M_6}{2}\right)\dot{I} + \dot{E}_0 \qquad (1)$$

with $$\dot{E}_0 = E_0 e^{j(\pi/2 - \pi/\tau\, x_0)} \tag{2}$$

where R = resistance per phase of inside or outside armature-windings
L = self inductance per phase of inside or outside armature-windings
M_2 = mutual inductance between neighbouring inside and outside armature-windings
M_4 = mutual inductance between inside and outside armature-windings of the same phase
M_5, M_6 = mutual inductance between inside and outside armature-windings of lagging and leading phases
$\dot{I}$ = vector of phase current
$\dot{E}_0$ = vector of induced voltage
E_0 = effective value of induced voltage
x_0 = mechanical load-angle
ω = $2\pi f$ = angular velocity
f = supply frequency

The active power P_o, power loss P_l and the reactive power P_Q for each LSM system are described as follows:

$$P_o = 3E_0 I \sin\frac{\pi}{\tau}x_0 = F_x V_L \tag{3}$$

$$P_l = 6RI^2 \tag{4}$$

$$P_Q = 6\omega\left(L - M_2 + M_4 - \frac{M_5 + M_6}{2}\right)I^2 + 3E_0 I \cos\frac{\pi}{\tau}x_0 \tag{5}$$

where I = effective value of phase current
V_L = speed of launcher.

Apparent power P_a, the efficiency η and power factor $\cos\phi$ are thus calculated using equations (3) - (5).

$$P_a = \sqrt{(P_o + P_l)^2 + P_Q^{\,2}} \tag{6}$$

$$\eta = \frac{P_o}{P_o + P_l} \times 100 \tag{7}$$

$$\cos\phi = \frac{P_o + P_l}{P_a} \times 100 \tag{8}$$

Active electric energy E_M, electric loss energy E_l and energy-efficiency η_E are defined as follows:

$$E_M = \frac{1}{3600}\int_0^{t_M} P_o(t)dt \quad \text{(Wh)} \tag{9}$$

$$E_l = \frac{1}{3600}\int_0^{t_M} P_l(t)dt \quad \text{(Wh)} \tag{10}$$

$$\eta_E = \frac{E_M}{E_M + E_l} \times 100 \tag{11}$$

where t_M = total running time in seconds of the launcher which operates as a motor.

DESIGN OF POWER SUPPLY SYSTEM AND SECTION-LENGTH

Especially for the H-II rocket which is 220 times heavier than the rocket in previous papers [1], [2], power supply system design is one of the most important problems in reducing reactive power at a peak speed of 900 km/h as much as possible. By increasing number of power supply systems, one section-length of the long-stator along the guideway is made shorter, so that a large component of reactive power which is expressed by the first term in the right hand side of equation (5) is decreased in propotion to section-length. But with its increase, the total initial cost also increases. We have designed four-power supply (A-B-C-D) system which has four sets of inverters.

The section-length depends strongly on launcher speeds. Before the launcher enters the next section, the armature-current in the section is required to be at a steady state. The time constant is the same in all sections, so that the higher the speed of launcher increases, the longer one section-length should be. Figure 3 shows a design of total section-length which includes the 5 groups with 18-, 30-, 39-, 42- and 36-m-sections. The five kinds of section-lengths are determined considering the time (170 ms) required to converge switch-on transient phenomena, which is about three times larger than the time constant τ_c = 55.5 ms as shown in Table 1. Tables 2 and 3 is for (A-B) and (A-B-C) systems.

Table 1. Resistance, inductances and time constant in each section for four-power-supply (A-B-C-D) system

section / paramater	group (1) 6 sections of 18-m-section	group (2) 10 sections of 30-m-section	group (3) 8 sections of 39-m-section	group (4) 10 sections of 42-m-section	group (5) 10 sections of 36-m-section
R (Ω)	0.0706	0.1176	0.1529	0.1646	0.1411
$L - M_2 + M_4$ (mH)	3.936	6.560	8.528	9.184	7.872
$M_5 + M_6$ (mH)	0.0362	0.0604	0.0785	0.0846	0.0725
τ_c (ms)	55.5	55.5	55.5	55.5	55.5

Table 2. Resistance, inductances and time constant in each section for two-power-supply (A-B) system

section / parameter	group (1) 3 sections of 36-m-section	group (2) 5 sections of 60-m-section	group (3) 4 sections of 78-m-section	group (4) 5 sections of 84-m-section	group (5) 5 sections of 69-m-section
R (Ω)	0.1529	0.2352	0.3058	0.3293	0.2705
$L - M_2 + M_4$ (mH)	8.528	13.120	17.056	18.368	15.088
$M_5 + M_6$ (mH)	0.0785	0.1208	0.1570	0.1691	0.1389
τ_c (ms)	55.5	55.5	55.5	55.5	55.5

Table 3. Resistance, inductances and time constant in each section for three-power-supply (A-B-C) system

section / parameter	group (1) 5 sections of 27-m-section	group (2) 7 sections of 39-m-section	group (3) 7 sections of 54-m-section	group (4) 7 sections of 57-m-section	group (5) 7 sections of 45-m-section
R (Ω)	0.1058	0.1529	0.2117	0.2234	0.1764
$L - M_2 + M_4$ (mH)	5.904	8.528	11.808	12.464	9.840
$M_5 + M_6$ (mH)	0.0544	0.0785	0.1087	0.1148	0.0906
τ_c (ms)	55.5	55.5	55.5	55.5	55.5

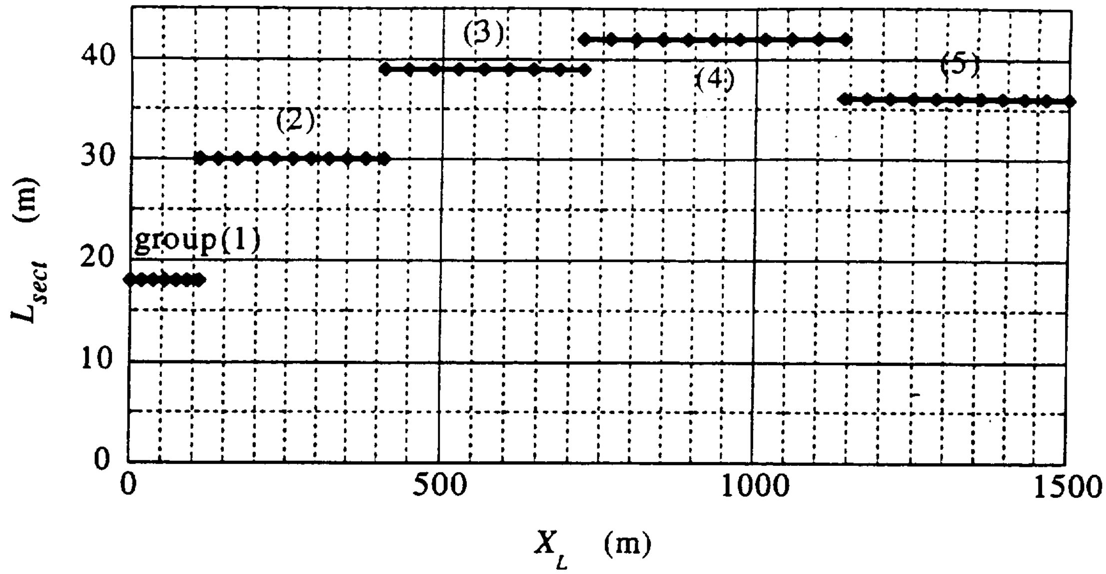

Figure 3. The 44 sections divided into five groups along the guideway

NUMERICAL EXPERIMENTS

The superconducting LSM rocket launcher system (see Table 4) is designed for the 1-ton rocket to attain a speed of 700 km/h at the height of 100 m above the ground. In the limited length of LSM armature guide tube, the linear launcher is controlled to meet the command acceleration pattern. It has the 6.6-s-acceleration-phase with a quick variation from zero to 4 G's for 0.5 s and 4 G's kept for 6.1 s, and the 4.67-s-deceleration-phase with a very quick variation from 4 G's to -7.5 G's for 1.3 s, -7.5 G's kept for 2.87 s and a very quick variation from -7.5 G's to zero for 0.5 s.

Table 4. Design data of superconducting LSM rocket launcher.

Guide Tube :		Total weight	15 ton
Total length	1,500 m	No. of Superconducting Magnets	60
Diameter	7 m	Superconducting Magnets per one LSM :	
LSM Armature Guide Tube :		No. of poles	15
Total length	1,500 m	Coil length	1.3 m
Inside diameter	5.0 m	Coil width	0.5 m
Outside diameter	5.1 m	MMF	700 kAT
No. of LSM Armature	4	Pole pitch	1.5 m
Coil length	0.8 m	Rocket :	
Coil width	0.6 m	Total weight	220 ton
Linear Launcher :		Clearance Gap :	
Total length	23 m	Electrical gap between coil centers	25 cm
Diameter	4.8 m	Mechanical gap	10 cm

Simulated Motions of LSM Launcher and Rocket

Figure 4 (a) and (b) show that the rocket is released from the launcher just after the peak speed at the height of 1,000 m from guideway tube bottom and launches with an initial speed of about 900 km/h. After the rocket ascends freely, receiving lateral force due to the Coriolis force in the guide tube, it flies out the LSM guide tube with a speed of about 720 km/h and then attains the command speed of 700 km/h at the height of 100 m above the ground. An instance at which the rocket is released is known from an instance for $\Delta H = 0$ in Fig. 4 (e). As shown in Fig. 4 (c), the launcher is controlled to follow very well the command acceleration pattern according to the command mechanical load-angle in Fig. 4 (f). The required armature-current and thrust force are shown in Figs. 4 (g) and (j).

Figure 4 (l) shows that the Coriolis force in the Z-direction is compensated completely using the guidance force in Fig. 4 (k) before the release point and after that the launcher itself is controlled quickly and stably in the center of the LSM guide tube. On the other hand the rocket is deflected in the reverse direction of the Z-axis, *i. e.* in the westward direction, by 3.75 cm at the flying-out point of the guide tube end. The deflection is sufficiently small compared with a mechanical clearance between the rocket and the inside coil of LSM armature, such that the rocket does not come into collision with the wall of the inside coils illustrated with shade in Fig. 4 (l). Figure 4 (l) shows that the launcher makes no motion in the Z-direction and the rocket is moved quite slowly in the westward direction due to the Coriolis force.

Electrical Dynamics Simulations

Figure 5 shows simulated results for terminal voltage, active-, reactive- and apparent-powers, power loss, efficiency and power factor per LSM for three cases of the power supply systems. They are power-supply system (PSS) (A-B), (A-B-C) and (A-B-C-D) which have two sets, three sets and four sets of inverters per LSM, respectively. Each terminal voltage per phase becomes a maximum value of 168 kV, 117kV and 93kV at a peak speed of 900 km/h, as shown in Fig. 5 (a). By using PSS (A-B-C-D) with four sets of inverters, the maximum voltage can be decreased to half value as compared with that of PSS (A-B) with two sets of inverters. The maximum active (output) power of about 1 GW is required as shown in Fig. 5 (b). Even in PSS (A-B-C-D), it is followed by the maximum power loss of 60 MW in Fig. 5 (c) and the maximum reactive power of 1.9 GVar in Fig. 5 (d) which result in the maximum apparent power of 2.4 GVA in Fig. 5(e). However, very high efficiency of above 90 % is obtained during almost all operating phases of LSM launcher controlled by PSS (A-B-C-D), as shown in Fig. 6 (a). Power factor is also generally very high and its minimum value is above 50 % in Fig. 6 (b) especially in PSS (A-B-C-D).

According to equations (9), (10) and (11), active electric-energy E_M, power loss energy E_l and energy-efficiency η_E are calculated as shown in Table 5. Active electric-energy E_M due to active power P_o shown in Fig. 5 (b) is constant independently of three kinds of power supply systems. Its value is very small though the maximum power at the peak speed of 900 km/h is extremely high. It is due to very short operating time of about 12 s. Power loss energy E_l is much smaller than electric-energy E_M and strongly dependent on three kinds of power supply systems as shown in Table 5, because the section-length and the armature coil resistance become smaller corresponding to PSS (A-B), (A-B-C) and (A-B-C-D). Consequently, energy-efficiency η_E is generally very high. Especially in PSS (A-B-C-D) very high value of 95 % is obtained.

Table 5. Active electric-energy, Power loss energy and energy-efficiency for three kinds of PSS

energy \ PSS		(A-B)	(A-B-C)	(A-B-C-D)
E_M	(kWh)	929.45	929.45	929.45
E_l	(kWh)	98.47	66.29	48.95
η_E	(%)	90.42	93.34	94.99

CONCLUSIONS

A vertical type superconducting LSM rocket launcher system under the ground which is operated in an attractive-mode is proposed to apply to full-size H-II rocket with the first acceleration rocket eliminated. To reduce maximum terminal phase-voltage and maximum reactive power and to improve efficiency and power factor, three kinds of power-supply systems with two sets, three sets and four sets of inverters are designed and evaluated for feasibility study.

The following results are obtained from the simulation study:

(1) The novel armature-current control method proposed previously by us was successfully applied in an attractive-mode operation for the 15-ton-launcher with 220-ton-rocket to meet the 4 G acceleration pattern and for the launcher without the released rocket to meet 7.5 G deceleration pattern. The launcher is controlled quite stably with no deflection in the center of the guide shaft with compensating for the Corioli's force as a lateral disturbance force.

(2) Even when the designed power-supply (A-B-C-D) system with four sets of inverters is used and electric characteristics are improved to a large extent, the maximum terminal phase-voltage is about 90 kV, the maximum active (output) power about 1 GW, the maximum power loss 60 MW, the maximum reactive power 1.9 Gvar and the maximum apparent power 2.4 GVA for each LSM.

(3) But efficiency is generally very high and power factor is also above 50 %. Active electric-energy is only 930 kWh, electric loss energy is only about 49 kWh which is about 5 % as compared with electric-energy, and very high energy-efficiency of 95 % is obtained.

(4) The LSM rocket launcher system requires very high initial cost but relatively low operating cost. The launcher system is feasible technically.

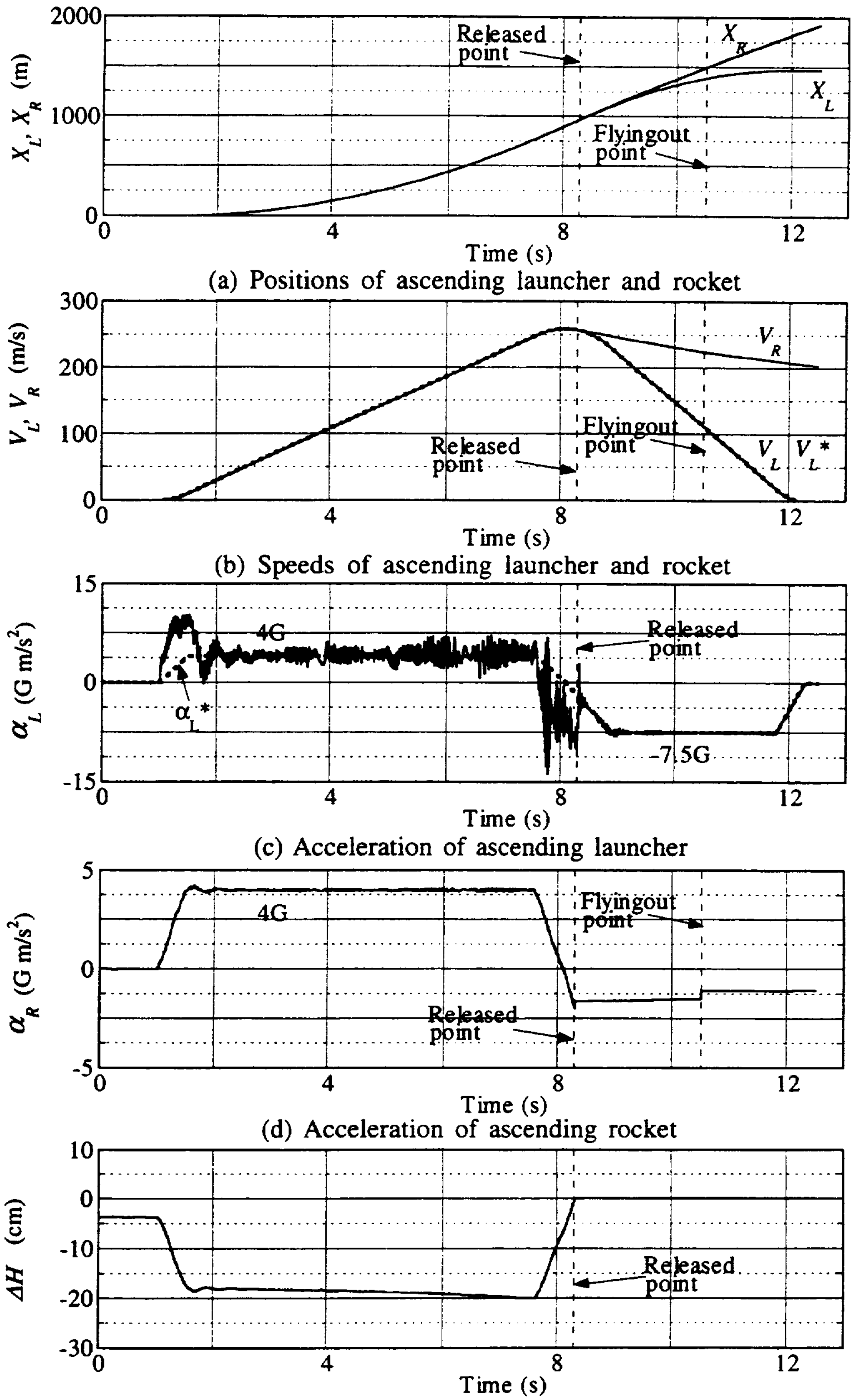

(a) Positions of ascending launcher and rocket

(b) Speeds of ascending launcher and rocket

(c) Acceleration of ascending launcher

(d) Acceleration of ascending rocket

(e) Relative height between launcher and rocket

Figure 4. Ascending motion of LSM rocket laucher

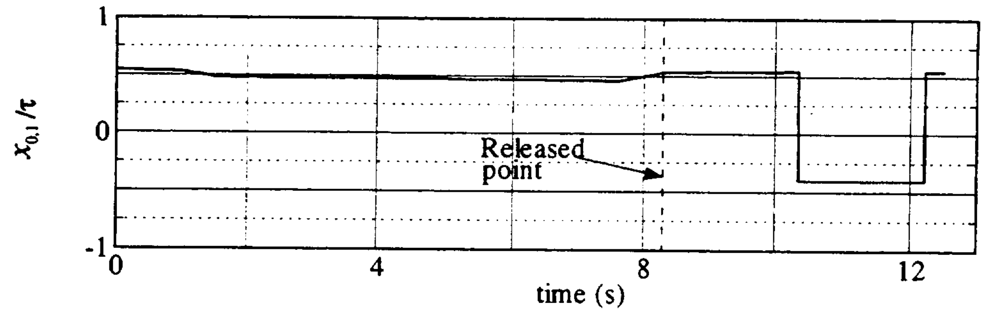

(f) Mechanical load-angle of inside armature winding

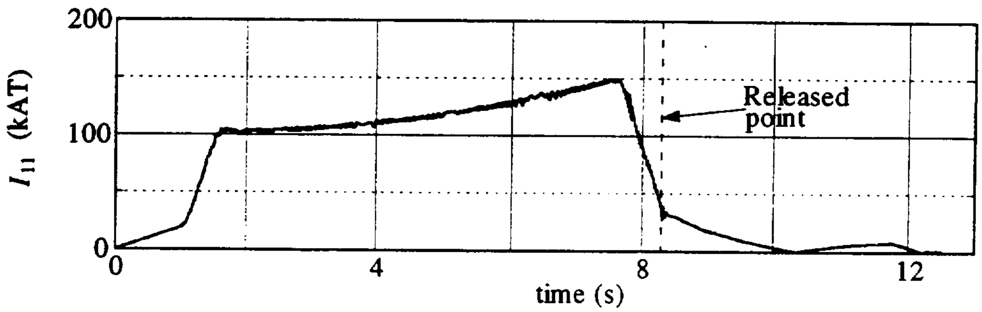

(g) Current of inside armature-winding in LSM①

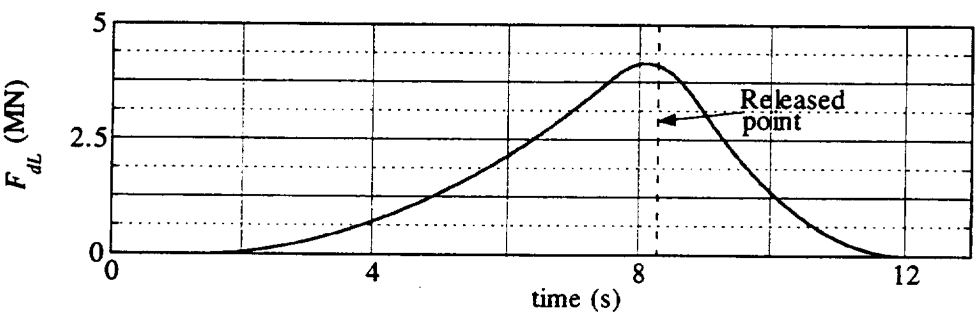

(h) Aerodynamic drag acting on launcher

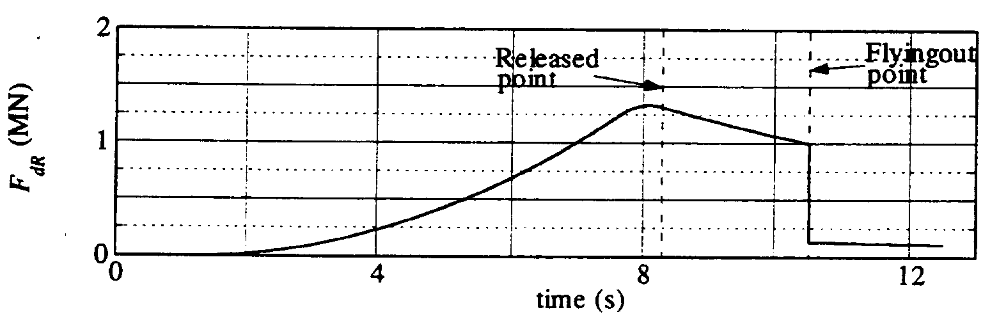

(i) Aerodynamic drag acting on rocket

Figure 4. Ascending motion of LSM rocket launcher

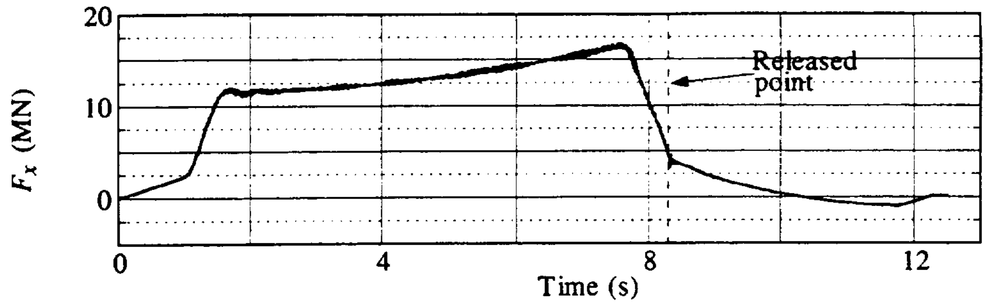

(j) Total thrust force in the X-direction

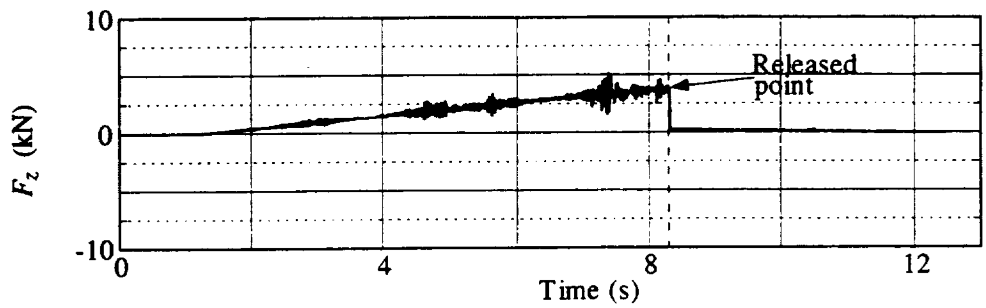

(k) Total guidance force in the Z-direction

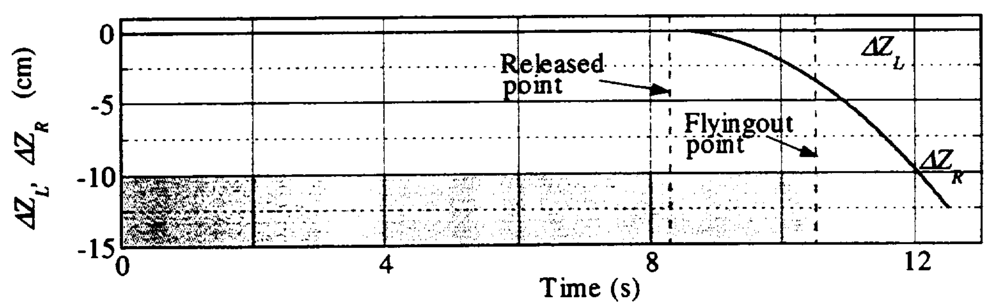

(l) Laucher and rocket deflections in the Z-direction

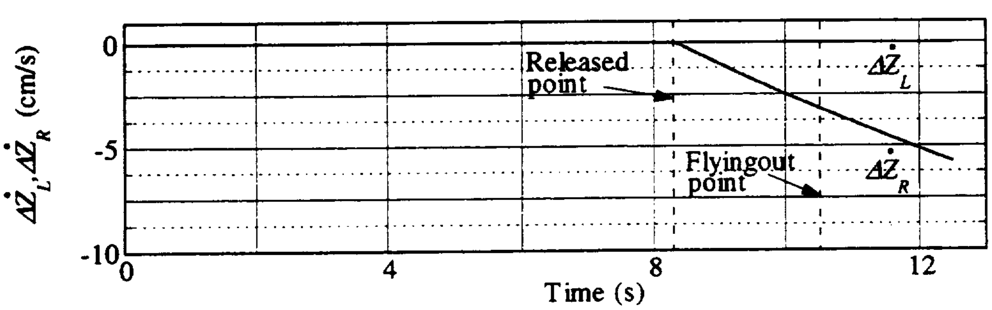

(m) Laucher and rocket speeds in the Z-direction

Figure 4. Ascending motion of LSM rocket launcher (cont.)

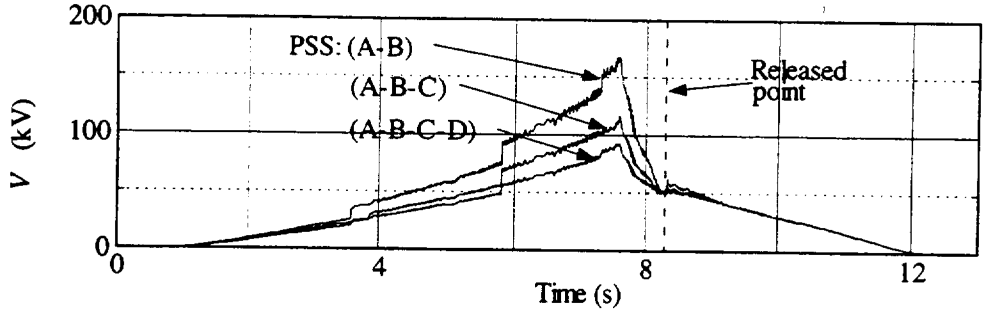

(a) Terminal voltage per phase

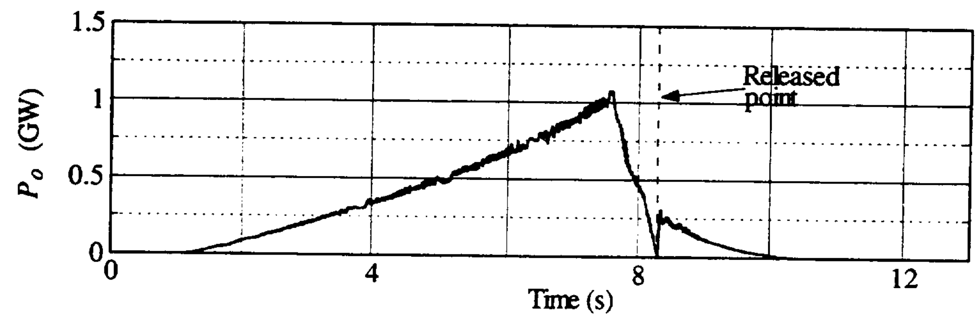

(b) Active power

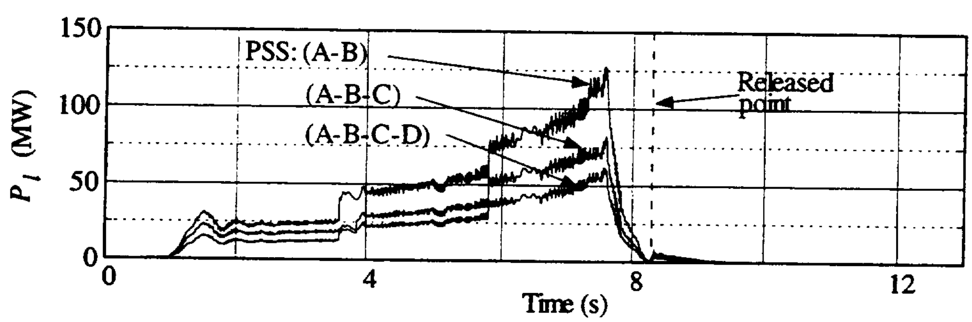

(c) Power loss

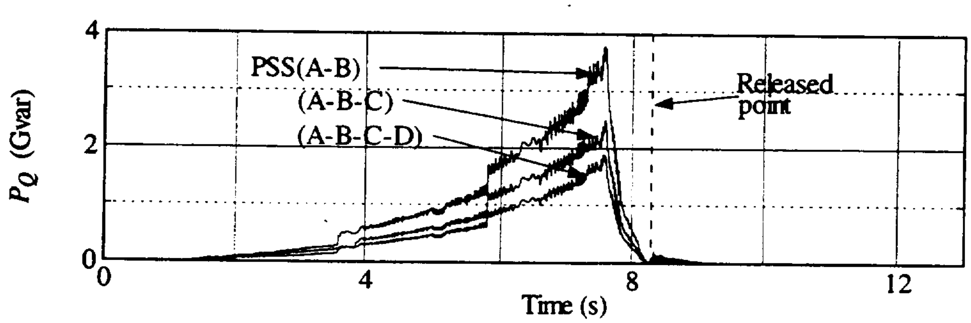

(d) Reactive power

Figure 4. Ascending motion of LSM rocket launcher (cont.)

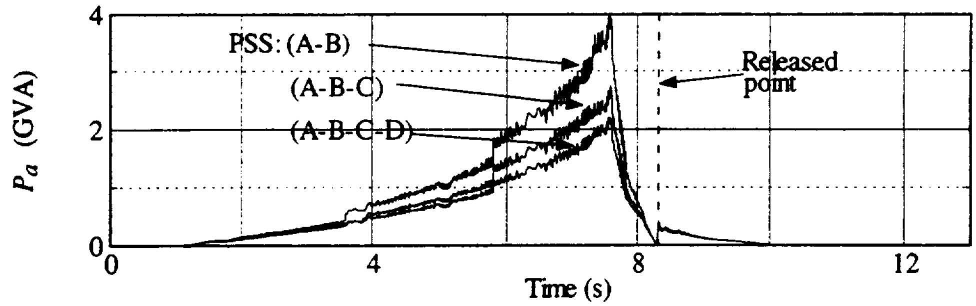

(e) Apparent power

Figure 5. Terminal voltage and electric powers in three kinds of power supplies

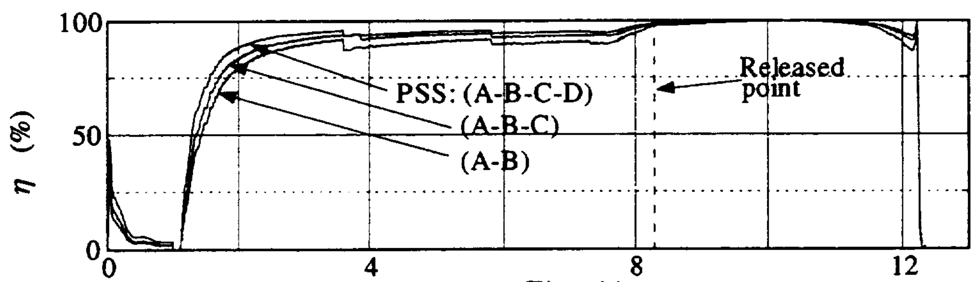

(a) Efficiency

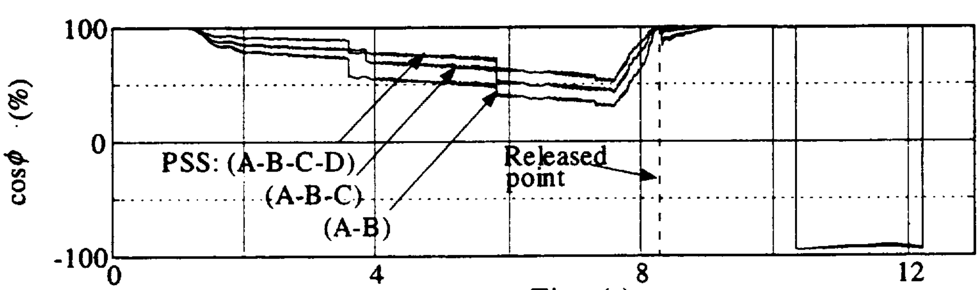

(b) Power factor

Figure 6. Efficiency and power factor for three kinds of power supplies

ACKNOWLEDGEMENTS

The authors gratefully acknowledge Mr. Yuji Asoh for his great help in making this paper.

REFERENCES

1. K. Yoshida, K. Hayashi and H. Takami : Electromechanical Dynamics of Superconducting LSM Rocket Launcher System in Attractive-Mode, NASA Conference Publication 3336 Part 2, July 1994, pp. 623 - 638
2. K. Yoshida, T. Ohashi, K. Shiraishi and H. Takami : Feasibility Study of Superconducting LSM Rocket Launcher System, NASA Conference Publication 3247 Part 2, May 1994, pp. 607 - 621
3. K. Yoshida, T. Ohashi, K. Shiraishi and H. Takami : Dynamics Simulations of Superconducting LSM Rocket Launcher System, J. of Space Tech. and Science, Vol.9 No.2, Autumn 1993, pp. 13 - 28
4. K. Yoshida, A. Kunihiro and T. Ohhashi : Superconducting LSM Dynamics in Ground - Based Zero - Gravity Facility, Proc. of Inter. Conf. on the Evolution and Modern Aspects of Synchronous Machines, Zurich, Aug. 1991, Part 3, pp. 797 - 802